

# Deformation and Energy-Absorption Characteristics of Microcellular EPDM Rubber

KRISHNA CHANDRA GURIYA, D. K. TRIPATHY

Rubber Technology Centre, I.I.T., Kharagpur - 721302, India

Received 18 February 1997; accepted 4 September 1997

**ABSTRACT:** Compressive stress-strain properties of closed-cell microcellular EPDM rubber vulcanizates with and without a filler were studied with the variation of density. For filler variation studies, silica and carbon black (N330) were used. With a decrease in density, the stress-strain curve for microcellular EPDM behaves differently from that for the solid vulcanizates: The curve rises steeply when cell breakdown occurs. The compressive stress-strain properties are found to depend on the strain rate. The compression set at constant stress increases with decreasing density. The energy-absorption behavior was studied from the compressive stress-strain properties. The efficiency,  $E$ , and ideality,  $I$ , parameters were also determined as they are useful for the evaluation of closed-cell microcellular rubber as a cushioning and packaging material. These parameters were plotted against stress to find the maximum efficiency and maximum ideality region which will make these materials suitable for cushioning or packaging applications. © 1998 John Wiley & Sons, Inc. *J Appl Polym Sci* 68: 263–269, 1998

**Key words:** microcellular rubber, EPDM, compressive stress-strain, energy absorption

## INTRODUCTION

Flexible cellular polymers have a growing range of engineering applications and are used as cushioning materials for the protection of fragile products during handling and transportation. The compressive stress-strain, shock, and vibration transmissibility characteristics are important for the design of energy-absorbing structures. The mechanism of deformation in cellular polymer was studied for compression by several authors.<sup>1–8</sup> The stress-strain properties depend upon the cell structure of the cellular polymer, that is, whether the cells are open or closed. In closed-cell polymers, two components normally contribute to the modulus value in compression<sup>9–11</sup>: The first is due

to the deformation of cell structure, and the second is caused by the buildup of pressure within the closed cell. The mechanical properties of cellular polymers, used as cushioning and packaging materials, have been studied from stress-strain curves in compression.<sup>12</sup> Williams reported the compression modulus and mathematical modeling for microcellular foams.<sup>13</sup> Polymeric foams possess properties that make them applicable as shock and vibration dampers. They can undergo large compressive deformation and absorb significant amounts of energy during a deformation cycle. Cellular and microcellular rubber differ greatly in their cushioning ability. The energy-absorption characteristics of cellular plastics and rubber have been determined by several authors.<sup>14,15</sup> The energy-absorption characteristics of cellular foams have been evaluated by efficiency and ideality parameters.<sup>12,16</sup>

In the present study, compressive stress-strain properties of closed-cell microcellular EPDM with several blowing agent loadings in

Correspondence to: D. K. Tripathy.

Contract grant sponsor: Council of Scientific and Industrial Research, Government of India.

*Journal of Applied Polymer Science*, Vol. 68, 263–269 (1998)

© 1998 John Wiley & Sons, Inc.

CCC 0021-8995/98/020263-07

**Table I Formulation of the Mixes**

	Mix No.										
	G <sub>10</sub>	G <sub>12</sub>	G <sub>14</sub>	GS <sub>20</sub>	GS <sub>22</sub>	GS <sub>24</sub>	GS <sub>26</sub>	EB <sub>20</sub>	EB <sub>22</sub>	EB <sub>24</sub>	EB <sub>26</sub>
EPDM	100	100	100	100	100	100	100	100	100	100	100
Silica	—	—	—	30	30	30	30	—	—	—	—
Carbon black	—	—	—	—	—	—	—	30	30	30	30
Paraffin oil	2	2	2	9	9	9	9	4.5	4.5	4.5	4.5
DNPT	0	2	4	0	2	4	6	0	2	4	6

Each mix contains ZnO, 2 phr, St. acid, 2 phr, and DCP, 2 phr.

gum and silica-, and carbon black-filled vulcanizates were studied. Strain-rate dependency in compression and compressive permanent set at constant stress was also studied. The energy-absorption characteristics of the closed-cell microcellular rubber were evaluated by the efficiency of energy absorption, and ideality parameters<sup>12,16</sup> were obtained from the stress-strain curves.

## EXPERIMENTAL

### Materials Used

EPDM rubber (Kelton 520, ethylene content 55 mol %, diene content 4.5 mol % [DCPD], specific gravity 0.86, manufactured by DSM Chemicals, Holland) was used. The precipitated silica used as a filler is manufactured by Degussa AG, Germany. Its characteristics are as follows: specific gravity, 2.0; BET surface area, 120–160 m<sup>2</sup> g; and particle size, 10–20 nm. HAF Black (N330) used as a filler is manufactured by Phillips Carbon Black, India. The dicumyl peroxide (DCP) used was Percidol 540C (40% DCP on an inert filler), manufactured by Chemoplast (I) Ltd. Dinitrosopentamethylene tetramine (DNPT) used as a blowing agent is manufactured by High Polymer Labs, India.

### Compounding and Sample Preparation

The rubber was compounded with other ingredients according to the formulations of the mixes (Table I) in a two-roll mill and the blowing agent was added at the end in the cold-roll mill. The compounds were molded at 160°C, to 80% of their respective maximum cure times, in an electrically heated hydraulic press. All sides of the mold were given a taper at 30° to facilitate the expansion of the microcellular rubber and to achieve better

mold release. The expanded microcellular sheets were postcured at 100°C for 1 h in an electrically heated oven.

### Physical Testing

The cylindrical samples were cut from the microcellular sheet for compression stress-strain properties according to the ASTM D575-81 standard. For testing the solid vulcanizates, the samples were directly molded according to the ASTM D575-81 standard. For the measurement of the compression set at constant stress, the ASTM D395-78 standard method was used. The cylindrical samples were compressed at 440 lb in.<sup>2</sup> stress for 24 h at room temperature. After release of the stress, the equilibrium thickness was measured for each specimen.

## RESULTS AND DISCUSSION

### Mechanical Properties in Compression

The stress-strain properties of silica-filled compounds in compression, at various levels of blowing agent loading, are shown in Figure 1. The increase of stress with strain for microcellular rubber is found to be different from that for solid rubber. The initial increase of stress is found to be slow for microcellular rubber compared to that of the solid rubber, but after a certain strain, the stress increases steeply. The microcellular rubbers used have a closed-cell structure.<sup>17,18</sup> At medium compressive strain, buckling of the cell structure is intensified. The compressive strain also accelerates the gas pressure buildup. At higher gas pressure, cell walls break and collapse. After this stage, the compressive stress increases rapidly, since all cells have collapsed, leaving a bulk solid rubber rather than a closed-cell micro-

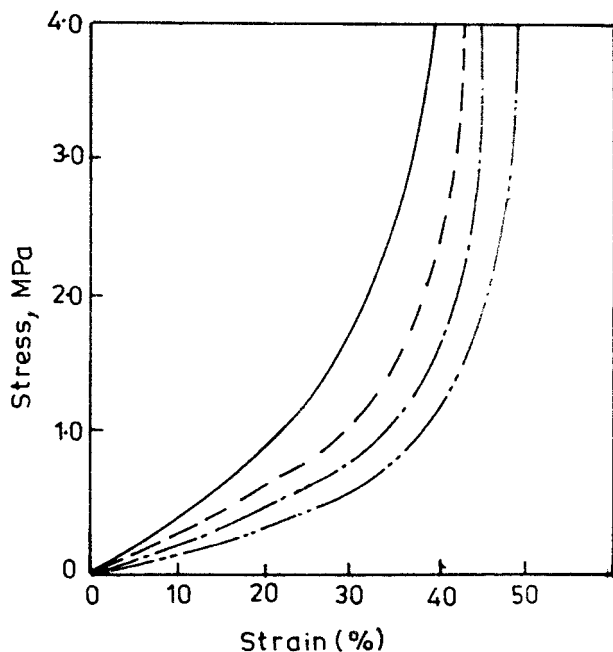


**Figure 1** Compressive stress-strain curves of 30 phr silica-filled solid and microcellular gum EPDM rubber vulcanizates: (—) GS<sub>20</sub> (density, 0.97); (---) GS<sub>22</sub> (density, 0.83); (- · -) GS<sub>24</sub> (density, 0.80); (- · · -) GS<sub>26</sub> (density, 0.67).

cellular rubber. Figure 1 shows the different curves corresponding to the variation in blowing agent concentration, that is, density. The moduli of silica-filled vulcanizates, as well as gum and carbon black-filled microcellular rubber vulcanizates, at different percentages of strain and density, are given in Table II. It is found that with increase in the blowing agent loadings, the modulus values decrease, which is obviously due to the reduction in solid rubber content. Figure 2 describes the effect of different filler loadings at 4 phr blowing agent loading.

The relative modulus ( $\sigma_f/\sigma_s$ ) at 10 and 20% strain is plotted against relative density ( $\rho_f/\rho_s$ )

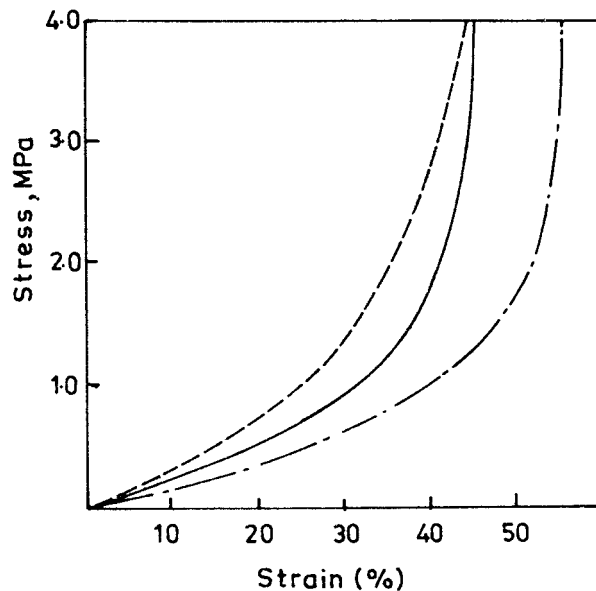


**Figure 2** Compressive stress-strain curves of gum and silica- and carbon black-filled microcellular EPDM rubber vulcanizates at 4 phr blowing agent loading: (---) EB<sub>24</sub> (density, 0.85); (—) GS<sub>24</sub> (density, 0.80); (- · -) G<sub>14</sub> (density, 0.79).

in Figure 3. The logarithmic plots show that the relative modulus decreases with decrease in the relative density or volume fraction of the rubber.

### Compression Rate

The compressive stress-strain curves of gum and silica-, and carbon black-filled vulcanizates at different strain rates are shown in Figure 4. The figure shows that the closed-cell microcellular rubbers are strain rate-dependent. The stress-strain curve becomes steeper the higher the strain rate. The effect of gas on the stress-strain curve of closed-cell microcellular elastomeric foams is much more pronounced. An additional strain-rate dependence is caused by the transition

**Table II** Physical Properties of Closed-cell Microcellular EPDM in Compression

	Mix No.										
	G <sub>10</sub>	G <sub>12</sub>	G <sub>14</sub>	GS <sub>20</sub>	GS <sub>22</sub>	GS <sub>24</sub>	GS <sub>26</sub>	EB <sub>20</sub>	EB <sub>22</sub>	EB <sub>24</sub>	EB <sub>26</sub>
10% modulus (MPa)	0.35	0.30	0.18	0.40	0.33	0.26	0.20	0.87	0.62	0.35	0.25
20% modulus (MPa)	0.75	0.63	0.49	1.02	0.73	0.51	0.35	1.61	1.17	0.72	0.47
Density (g cm <sup>3</sup> )	0.89	0.83	0.79	0.97	0.83	0.80	0.67	1.06	0.90	0.85	0.71
Relative density ( $\rho_f/\rho_s$ )	1.00	0.94	0.89	1.00	0.85	0.81	0.68	1.00	0.84	0.79	0.71
Permanent set (%)	7.5	9.0	15.7	9.0	16	35	45	7.5	12	28	37

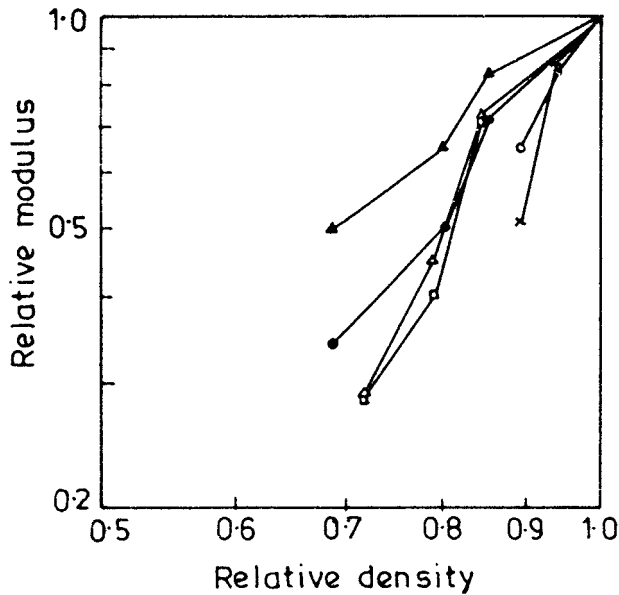


**Figure 3** Logarithmic plots of relative modulus ( $\sigma_f/\sigma_s$ ) versus relative density ( $\rho_f/\rho_s$ ). Unfilled: (x) 10% modulus; 20% (○) modulus, 30 phr silica-filled: (▲) 10% modulus; (●) 20% modulus, 30 phr carbon black-filled: (□) 10% modulus; (△) 20% modulus.

from isothermal to adiabatic compression of the gas itself as the strain increases. But as Zhang and Ashby<sup>19</sup> pointed out, the gas is always isothermal because of its intimate contact with the cell wall which has a thermal capacity higher than that of the gas. So, the strain-rate dependence of the closed-cell microcellular rubber can be derived directly from that of the cell wall material.

**Compression Set**

Compression-set properties of closed-cell microcellular gum and filled rubber vulcanizates at constant stress are given in Table II. It is observed that, with in the increase blowing agent loading, that is, decreasing density, the permanent set increases. With decreasing density, the number of cells increases and the cell wall becomes thin. Hence, the deformation at constant stress increases. So, the breakdown of the closed-cell wall increases, leading to an increase in set properties.

**Energy-absorption Characteristics**

The energy-absorption characteristics are determined from static slow-rate compression measurements. To evaluate and compare the perfor-

mance and suitability of the energy absorption of different closed-cell microcellular rubbers, two parameters were defined.<sup>12,16</sup> These parameters are called the efficiency of energy absorption or efficiency,  $E$ , and the ideality parameter,  $I$ . The efficiency is defined as the ratio between the energy absorbed by a microcellular rubber compressed to a maximum strain,  $\epsilon_m$ , and that absorbed by an ideal microcellular rubber that transmits the same maximum (but constant) stress,  $\sigma_m$ , to the product when fully compressed. Thus,

$$E = \frac{Ah \int_0^{\epsilon_m} \sigma d\epsilon}{Ah \sigma_m 1} = \frac{\int_0^{\epsilon_m} \sigma d\epsilon}{\sigma_m} \tag{1}$$

where  $h$  is the thickness of the microcellular rubber and  $A$  is the contact area.

The ideality parameter,  $I$ , is defined as the ratio between the energy absorbed by an actual and an ideal cushioning material compressed to the same strain, namely:

$$I = \frac{Ah \int_0^{\epsilon_m} \sigma d\epsilon}{Ah \sigma_m \epsilon_m} = \frac{\int_0^{\epsilon_m} \sigma d\epsilon}{\sigma_m \epsilon_m} \tag{2}$$

From the stress-strain curves (Figs. 1 and 2)

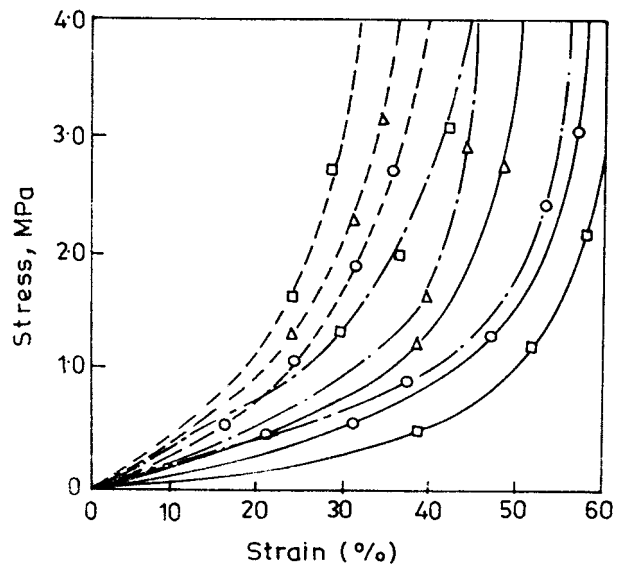


**Figure 4** Compressive stress-strain curves of gum and filled microcellular rubber vulcanizates at different strain rates: (—)  $1.66 \times 10^{-3}$  s; (---)  $3.33 \times 10^{-2}$  s; (- -)  $3.33 \times 10^{-1}$ /s. (○) G<sub>14</sub> (density, 0.79); (△) GS<sub>24</sub> (density, 0.80); (□) EB<sub>24</sub> (density, 0.85).

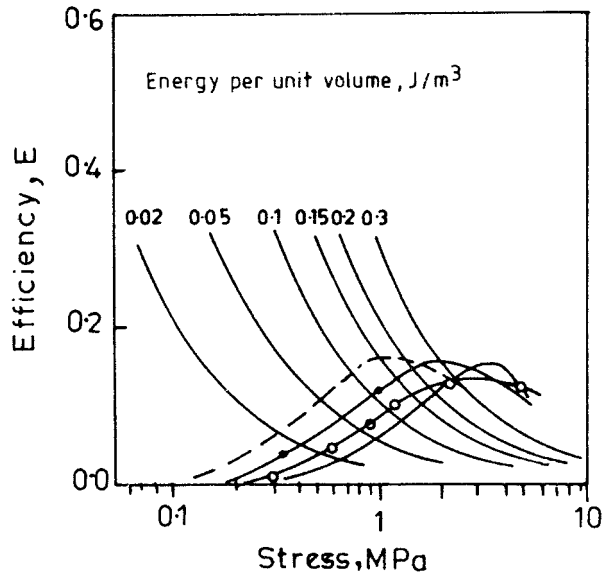


**Figure 5** Efficiency of energy absorption,  $E$ , of 30 phr silica-filled solid and microcellular EPDM rubber vulcanizates calculated from static experiment. (—) GS<sub>20</sub> (density, 0.97); (—○—) GS<sub>22</sub> (density, 0.83); (-·-) GS<sub>24</sub> (density, 0.80); (—) GS<sub>26</sub> (density, 0.67).

of silica-, gum and carbon black-filled closed-cell microcellular rubbers and with the help of eqs. (1) and (2), the efficiency,  $E$ , and ideality parameter,  $I$ , are calculated.

The efficiency of energy absorption,  $E$ , is plotted against the stress in Figure 5, corresponding to the silica-filled solid and microcellular rubber vulcanizates, respectively. The integrals in eqs. (1) and (2) are calculated from the experimental stress-strain curve using a computer program. It is seen that both solid and microcellular rubber show maximum efficiency at a different stress. With increase in the blowing agent loading, that is, with decreasing density, the maximum efficiency of the silica- and carbon black-filled system remains almost constant, but the maximum efficiency is at a lower stress. From eq. (1), it becomes evident that the product  $E\sigma_m$  is equal to the energy per unit volume that is absorbed by the microcellular rubber when compressed to the strain  $\epsilon_m$  and this product is a constant for a specific absorbed energy level.<sup>12,16</sup> Contours of constant energy levels are superimposed in Figure 5 for silica-filled compounds. Similar contours are also observed for carbon black-filled compounds. From these contours, it becomes evident that each microcellular rubber can absorb a different amount of energy at its maximum efficiency. With

decreasing density, for both silica- and carbon black-filled microcellular rubbers, the maximum efficiency curves become flat and the range of maximum efficiency becomes wider. Thus, the energy-absorption properties, that is, cushioning properties, become better. Figure 6 shows similar curves for different microcellular rubbers (with different fillers) at a 4 phr blowing agent loading.

The ideality parameter,  $I$ , is plotted in Figure 7 as a function of stress for silica-filled compounds. The ideality curve shows a maximum in silica-filled solid and microcellular rubber vulcanizates. It is observed that the maximum value is reached at a lower stress level than for the efficiency curve. The efficiency curves show maxima when the stress-strain curves start rising steeply, that is, where the closed cell is compressed and the rupture of cell walls starts and permanent set occurs. The stress level at which the maximum efficiency is reached is the criterion of choosing the maximum load for that closed-cell microcellular rubber in a cushioning application.<sup>16</sup> The ideality parameter,  $I$ , shows a maximum value in the region of the stress-strain curve where the bending, stretching, and compression of enclosed gas occurs. So, for evaluating the closed-cell microcellular rubber for efficient application in energy absorption, the maximum

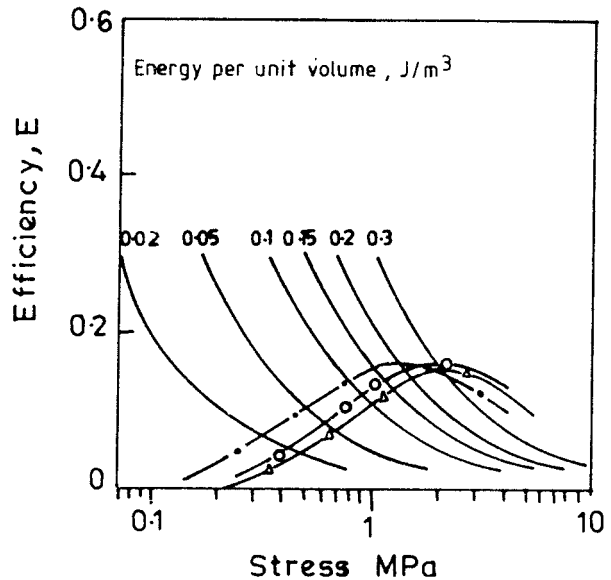


**Figure 6** Efficiency of energy absorption,  $E$ , of gum and silica- and carbon black-filled microcellular EPDM rubber vulcanizates at 4 phr blowing agent loading are calculated from static experiment. (—△—) EB<sub>24</sub> (density, 0.85); (—○—) GS<sub>24</sub> (density, 0.80); (-·-) G<sub>14</sub> (density, 0.79).

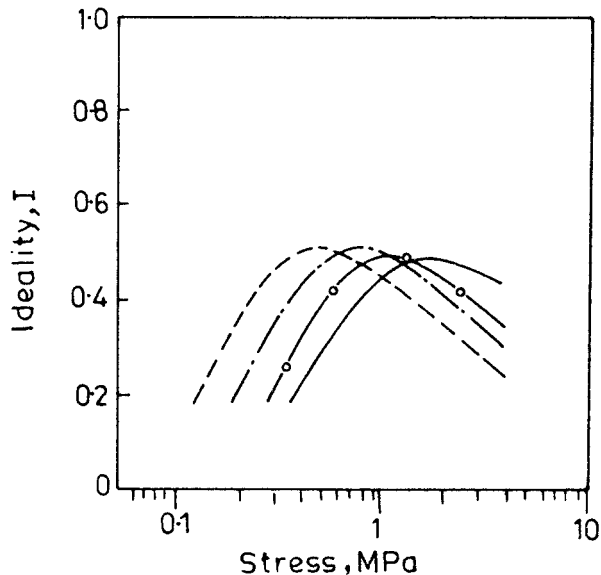


**Figure 7** Ideality,  $I$ , of 30 phr silica-filled solid and microcellular EPDM rubber vulcanizates calculated from static experiment. (—) GS<sub>20</sub> (density, 0.97); (—○—) GS<sub>22</sub> (density, 0.83); (-·-) GS<sub>24</sub> (density, 0.80); (---) GS<sub>26</sub> (density, 0.67).

ideality region is chosen. The nature of the ideality curve for carbon black-filled compounds is found to be similar to that of silica-filled compounds and, hence, is not shown.

### Energy-absorption Diagram

An approach which allows empiricism to be combined with physical modeling and which has attractive generality as a way of optimizing the choice of microcellular rubber, is offered by an energy-absorption diagram.<sup>20</sup> The procedure for constructing it from an experimental stress-strain curve is as follows: Figure 1 shows the stress-strain curves for microcellular rubber with various densities at a fixed strain rate and temperature. The area under each curve up to stress  $\sigma_p$  (stepping upward in  $\sigma_p$ ) gives the energy absorbed per unit volume  $W$ . The value of  $W$  is plotted against  $\sigma_p$  for each curve, normalizing both by the modulus of solid,  $E_s$ , measured at a strain rate of  $3.33 \times 10^{-2}$  s and a temperature of 25°C. The best microcellular rubber for a given package is the one that absorbs the most energy up to the maximum permitted package stress  $\sigma_p$ . Each microcellular rubber density has a  $\sigma_p$  for which it is the best choice given by the shoulder

on the energy curve (Fig. 8), because, here, the curve for that microcellular rubber lies above that of the other, the envelop of which describes a relationship between  $W$  and  $\sigma_p$  for the optimum microcellular rubber density. The envelope divides the diagram into an accessible region (below the line) and an inaccessible region (above). The equation of the line for silica-filled microcellular rubber (Fig. 8) is approximately given by

$$\frac{W}{E_s} = 0.19 \left( \frac{\sigma}{E_s} \right)^{1.175} \quad \text{for silica-filled compound}$$

Energy curves for gum and carbon black-filled compounds are constructed following the same procedure. The equations of the lines for gum and carbon black-filled microcellular rubber are found to be

$$\frac{W}{E_s} = 0.165 \left( \frac{\sigma}{E_s} \right)^{0.91} \quad \text{for gum compound}$$

$$\frac{W}{E_s} = 0.12 \left( \frac{\sigma}{E_s} \right)^{0.887}$$

for carbon black-filled compound

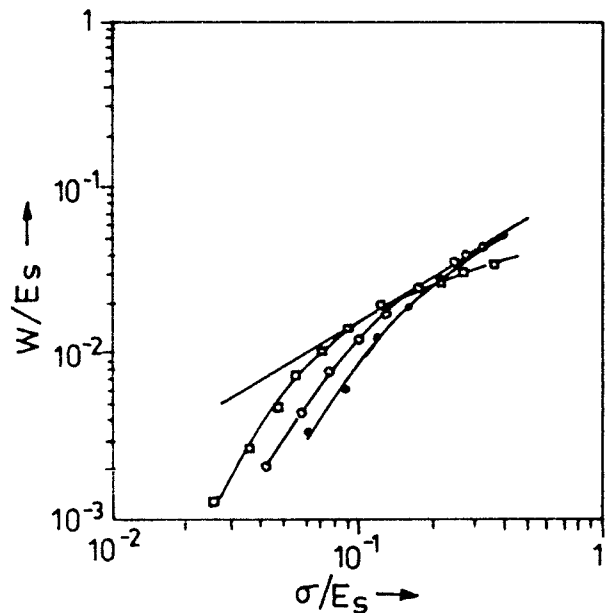


**Figure 8** An energy-absorption diagram of silica-filled microcellular rubber, constructed from static compressive stress-strain curve: (—●—) GS<sub>22</sub> (density, 0.83); (—○—) GS<sub>24</sub> (density, 0.80); (—□—) GS<sub>26</sub> (density, 0.67).

They are applicable for the relative density ( $\rho_r/\rho_s$ ), 0.89 to 0.94 for gum, 0.68 to 0.85 for silica, and 0.71 to 0.84 for carbon black-filled compounds.

## CONCLUSIONS

1. Compressive stress–strain curves of closed-cell microcellular gum and filled rubbers depend on the density. The nature of the stress–strain curve for microcellular rubber is different from that of the solid rubber vulcanizates.
2. The stress rises slowly against strain up to a certain level of applied strain, beyond which the stress rises quickly when the closed cell is fully compressed and the cell walls breaks down.
3. Compressive stress–strain properties are also dependent on the strain rate.
4. Compression set increases at constant stress with decreasing density.
5. Energy-absorption behavior is evaluated from the compressive stress–strain curve of microcellular rubber. The energy absorption efficiency,  $E$ , and ideality parameter,  $I$ , are found to play an important role in evaluating the energy-absorption characteristics of microcellular rubber.
6. The energy absorbed, per unit volume of microcellular rubber, depends on the density of the microcellular rubber as well as on the stress. From the energy-absorption diagram, it is observed that there is an optimum microcellular rubber density for a given packaging or energy-absorbing application.

We are grateful to the Council of Scientific and Indus-

trial Research, Govt. of India, for financial support for carrying out this investigation.

## REFERENCES

1. A. N. Gent and A. G. Thomas, *J. Appl. Polym. Sci.*, **1**, 107 (1959).
2. M. R. Patel and I. Finnie, *J. Mater.*, **5**, 909 (1970).
3. G. Gruenbaum and J. Miltz, *J. Appl. Polym. Sci.*, **28**, 135 (1983).
4. J. Miltz, O. Raman, and S. Mizrahi, *J. Appl. Polym. Sci.*, **38**, 281 (1989).
5. O. Raman, S. Mizrahi, and J. Miltz, *Polym. Eng. Sci.*, **30**, 197 (1990).
6. K. C. Rusch, *J. Appl. Polym. Sci.*, **14**, 1263 (1970).
7. L. J. Gibson and M. F. Ashby, *Proc. R. Soc. A*, **382**, 43 (1982).
8. J. T. Tsai, *Polym. Eng. Sci.*, **22**, 545 (1982).
9. A. N. Gent and A. G. Thomas, *Rubb. Chem. Technol.*, **36**, 597 (1963).
10. J. M. Lederman, *J. Appl. Polym. Sci.*, **15**, 693 (1971).
11. R. E. Skochdopole and L. C. Rubens, *J. Cell. Plast.*, **1**, 91 (1965).
12. J. Miltz and G. Gruenbaum, *Polym. Eng. Sci.*, **21**, 1010 (1981).
13. J. M. Williams, *J. Mater. Sci.*, **23**, 900 (1988).
14. E. A. Meinecke and D. M. Schwaber, *J. Appl. Polym. Sci.*, **14**, 2239 (1970).
15. K. C. Rusch, *J. Appl. Polym. Sci.*, **14**, 1433 (1970).
16. J. Miltz and O. Raman, *Polym. Eng. Sci.*, **30**, 129 (1990).
17. K. C. Guriya and D. K. Tripathy, *Plast. Rubb. Comp. Proc. Appl.*, **23**, 193 (1995).
18. K. C. Guriya and D. K. Tripathy, *J. Appl. Polym. Sci.*, to appear.
19. J. Zhang and M. F. Ashby, CPGS Thesis, Engineering Department, Cambridge, UK, 1988.
20. S. K. Maiti, L. J. Gibson, and M. F. Ashby, *Acta Metall.*, **32**, 1963 (1984).